Available online at www.sciencedirect.com
ScienceDirect
Journal of Nuclear Materials 363–365 (2007) 201–205
journal of nuclear materials
www.elsevier.com/locate/jnucmat

Measurements of the average energy of carbon atoms released from breakup of methane in the main SOL of DIII-D compared with DIVIMP code modeling

P.C. Stangeby [a,*], A.G. McLean [a], J.D. Elder [a], N.H. Brooks [b], W.P. West [b], D. Reiter [c]

[a] University of Toronto, Institute for Aerospace Studies, 4925 Dufferin Street, Toronto, Ont., Canada M3H 5T6
[b] General Atomics, San Diego, CA 92186-5608, USA
[c] Institut für Plasmaphysik Forschungszentrum, Jülich GmbH 52425, Jülich, Germany

Abstract

$^{13}CH_4$, $^{12}CD_4$ or $^{12}CH_4$ gases were puffed into the crown (top) of lower single-null divertor plasmas in DIII-D using toroidally symmetric injection, constituting a particularly simple experiment to interpret. The resulting CI (9094.83 Å) wavelength profiles were measured with a high resolution spectrometer. For a wide variety of plasma conditions, the shape of the profile was nearly constant, and could be approximately represented by a shifted gaussian distribution, corresponding to a temperature of the C-atoms of <1 eV. DIVIMP code analysis reported here, based on the recent Janev–Reiter database/model for methane breakup, has produced sufficiently close matches to these experimental CI profiles, to provide reasonable confidence that the controlling processes have been included.

Keywords: Carbon impurities; DIII-D; Hydrocarbons

1. Introduction

The detailed shape of the CI emission line contains information that, in principle, can be used to identify the relative contributions of chemical and physical sputtering from graphite plasma facing components. This paper reports spectroscopic measurements from methane – $^{13}CH_4$, $^{12}CD_4$, or $^{12}CH_4$ – puffing into the main scrape-off layer (SOL) in DIII-D, simulating chemical sputtering from the wall, which indicate that low average energy, $\lesssim 1$ eV, carbon atoms are released from the breakup of the injected gas in the edge plasma. Such low C-atom (CI) average energy was found over a range of discharge parameters studied in 30 plasma shots on 8 operating days. Since the C-atoms gain Frank–Condon energy from each stage of the molecular breakup process and also, while they are in charged fragments, experience heating due to collisions with deuterons, a more energetic C distribution might seem to be expected. As reported here, however, DIVIMP code modeling of the methane breakup using the recent

* Corresponding author. Fax: +1 858 455 4156.
E-mail address: stangeby@fusion.gat.com (P.C. Stangeby).

0022-3115/$ - see front matter © 2007 Elsevier B.V. All rights reserved.
doi:10.1016/j.jnucmat.2007.01.008

Janev–Reiter database [1,2] is found to replicate the measured CI wavelength profiles fairly closely – and better than the earlier Ehrhardt–Langer database [3] – indicating that the basic processes controlling methane breakup in a tokamak edge plasma have apparently now been identified.

2. Experiment

In these shots, $^{12,13}CH_4$ and $^{12}CD_4$ was injected toroidally symmetrically into the crown of lower single-null (LSN) plasmas, Fig. 1, at rates of ~3–20 Torr l/s in multiple, identical repeat shots in DIII-D. Such injection into the main SOL, rather than through a limiter or divertor target, avoids the complications of ongoing plasma interaction with deposits created by the methane injection, considerably simplifying the comparison with modeling and providing a better chance of achieving a definitive experimental test of breakup models. Injections were accomplished using a toroidally symmetric upper outer (cryo-pumping) plenum (with pump off) for a range of conditions: L- and H-mode; different densities; forward and reverse B_{tor}. Toroidal injection enjoys the further benefit that many of the edge diagnostics can be employed, e.g. to confirm that the plasma has not been perturbed, something that is considerably more difficult to achieve with local injection. In order to avoid perturbing the local plasma conditions, low injection rates were employed – ones that increased the local emissivity by less than a factor of 2 over the natural levels. The CI (9094.83 Å) line profile was measured using the high resolution multichord divertor spectrometer (MDS) viewing the crown region. Data were averaged over long (1–3 s) steady-state periods in each of a large number of repeat shots in order to compensate for low emission intensities. Higher puff rates would have produced stronger signals, but the low puff rates used, together with the toroidal nature of the injection, minimized the risk of perturbing the local plasma. The lack of perturbation was confirmed by the constancy of the radial profiles of n_e and T_e in the SOL, puff on/off, as measured by Thomson scattering near the injection location. The most intense CI signals were recorded for the MDS views closest to the injection point, Fig. 2. For a first, simple characterization of the CI profiles, they were fitted to a shifted Gaussian, with both the full-width-half-maximum (FWHM), and shift, being adjusted for best fit. The profiles were obtained by subtracting the pre-puff profile from the puff-on profile, with both profiles being averaged over at least 0.5 s. The average CI intensity was 3–10× less in L-mode than H-mode. Although a wide variety of plasma conditions were employed, remarkably little variation was found in the profiles and accordingly the data has been grouped as shown in Table 1; data for the most intense viewlines, 9, 11 and 12, were combined. Typically FWHM ~0.25 Å, corresponding to $T \sim 0.5$ eV for the emitting atoms.

Even when grouped in this way, the profiles differ by amounts less than the standard deviations, for the most part, the only exception being the different shifts for $^{13}CH_4$ and $^{12}CH_4$. For the H-mode this difference, $-0.097 - (-0.059) = -0.038 \pm 0.023$ Å, is consistent with the shift expected for the effect of the difference in masses between ^{13}C and ^{12}C on the finite-mass Rydberg constant, which is

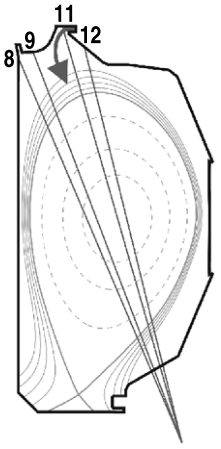

Fig. 1. Four viewing-lines of the spectrometer (MDS). Methane was injected toroidally symmetrically at the top of the vessel.

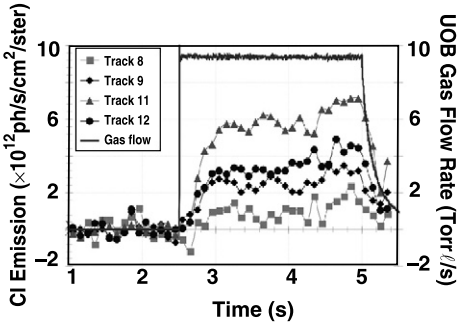

Fig. 2. Gas flow and integrated CI emission is shown vs time for a sample L-mode, reversed-B shot with puffing from the toroidal pumping plenum (UOB). The zero for the emission scale is set by the average pre-puff (2–2.5 s) values. Emission intensity comes to steady-state after ~0.5 s of gas flow due to the length of line between the gas supply and the vessel.

Table 1
Widths and shifts of the CI line

	FWHM L-mode	FWHM H-mode	Shift L-mode	Shift H-mode
$^{13}CH_4$	0.240 {4} (0.030)	0.253 {2} (0.027)	−0.043 {4} (0.022)	−0.097 {2} (0.016)
$^{12}CD_4$		0.269 {4} (0.039)		−0.024 {4} (0.015)
$^{12}CH_4$	0.253 {10} (0.022)	0.233 {4} (0.023)	−0.032 {10} (0.013)	−0.059 {4} (0.016)

Units (Å). Shifts are relative to the rest wavelength, 9094.83 Å. Number of shots in curly brackets. Standard deviations shown in round brackets. The experimental profiles include the effect of the MDS instrument function, for which FWHM ~0.20 Å.

−0.032 Å. Within larger error bars, the L-mode data are also consistent.

3. DIVIMP code modeling

Some of the experimental data were compared in detail with DIVIMP Monte Carlo code modeling of the multi-step fragmentation process for CH_4 molecules based on the model–database of Janev and Reiter [1,2]. As the C atom is followed by the code, an emission contribution for a specific spectroscopic diagnostic line of sight is calculated at each modeling time step – the velocity of the particle is used to calculate the Doppler shift in this emission contribution. The total emission from all simulation particles contributing to emission in the line of sight summed up for all time steps results in a wavelength profile for the modeled emission, which can be directly compared to the experimental measurements.

Franck–Condon energy is released by each breakup reaction. This energy is distributed inversely proportionally to the mass of the fragments and is applied in the center of mass frame for the molecular system. The energy release is typically 3D isotropic for the electron-induced breakup processes. Changes of molecular fragment state between neutrals and ions are also included. The 3D velocity of the neutrals is mapped to the local magnetic geometry with components parallel and perpendicular to the field line direction. While existing as an ion, the molecular fragment experiences heating collisions with the background plasma. At the end of this multi-stage process a C-atom is created with a 3D velocity dependent on its particular history. The simulation then follows many such particles (100 000 in the simulations presented here) and is then used to produce a CI line profile and also analysis of the particle speed and velocity distributions.

The modeling analysis was performed on a plasma background calculated for the $^{13}CH_4$ H-mode experiment [4]. On the setup day, a series of discharges were run to characterize the plasma into which $^{12}CH_4$ was puffed. The plasma profiles in the puff region were taken from nearby Thomson measurements of n_e and T_e in the SOL, neglecting parallel gradients in the crown SOL. These plasma profiles and the magnetic grid generated for shot 123 417 were then used for these simulations.

Fig. 3 shows the detailed comparison of the CI profile for the code and experiment. The code profiles incorporate the MDS instrument function, $f(\Delta\lambda) = 0.95e^{-(\Delta\lambda/0.1201)^2} + 0.05e^{-(\Delta\lambda/0.4204)^2}$, with $\Delta\lambda$ (Å), [5]. The experimental data used in Fig. 3 include all the H-mode data measured in the 2005 experiment [4], for the three most intense MDS Tracks, 9, 11 and 12; the ^{12}C data were not shifted, while the ^{13}C data were shifted by the finite-mass Rydberg difference of 0.032 Å. The match is quite good, indicating that the controlling processes have evidently been included in the Janev–Reiter (JR) model. A small discrepancy is discernable, possibly due to a small calibration wavelength error, ~0.02 Å.

The code was run to compare the JR, database for hydrocarbon breakup, and the older Ehrhardt–Langer, EL, database [3]. The JR database is more

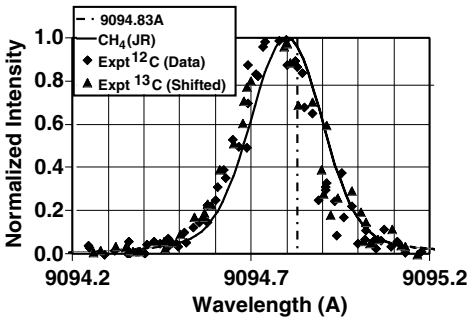

Fig. 3. Comparison of CI-9094.83 Å experimental and modeled line profiles. MDS Tracks 9, 11 and 12 data for all H-mode data from the 2005 $^{13}CH_4$ experiment and the previous set-up day that used $^{12}CH_4$. The ^{13}C experimental results have been shifted by 0.032 Å to account for differences between the base wavelength for this transition in ^{12}C and ^{13}C.

comprehensive, including about twice the number of breakup reactions as the EL one. This, plus differences in reaction cross sections between the two databases, results in much faster breakup occurring in the code for JR: using the JR (EL) databases for D, a C-atom on average experienced 4.15 (5.24) breakup reactions, gaining 1.17 (2.07) eV of Frank–Condon energy (i.e. from the potential energy of the methane molecule). The biggest difference, however, was that the breakup occurred so much faster for JR that the collisional heating (due to elastic collisions between D^+ and ionic HC-fragments) was only 0.61 eV, compared with 2.40 eV for EL. The final result was that the average kinetic energy of the C-atoms for JR was only 1.78 eV, compared with 4.48 eV for EL. Assuming the C-atom energy distributions were Maxwellian then from $\langle E\rangle = 3/2\,kT$, $T = 1.19$ (2.99) eV for JR (EL), which is a large part of the reason why the code analysis, for JR, closely matches the (cold) experimental result. The C-atom distribution was found to be non-Maxwellian, as can be noted from the high energy tail in Fig. 3. Fig. 4 shows the calculated speed distribution, compared with a Maxwellian distribution for $T = 0.4$ eV. The distribution cannot be fit very well by any Maxwellian, however, the bulk of the atoms can be approximated by a Maxwellian of energy ~0.5 eV, and these atoms tend to set the FWHM of the CI line. These two aspects, then, are the main reasons that the modeling result, based on the JR database, agrees rather well with the experiment.

Recently, the computer code HYDKIN (Reaction kinetics analysis online for hydrocarbon catabolism in hydrogen plasmas) has been made universally accessible, http://www.eirene.de/eigen/index.html. This code enables the user to easily examine the effects of launching any of a wide variety of hydrocarbon molecules into plasma of specified (spatially constant) density and temperature, specifying either the EL or JR database. No transport is included so HYDKIN cannot be directly compared with the DIVIMP analysis here, however, it can be readily used to help understand the results described above. For example, specifying plasma conditions representative of the region in the SOL where the DIVIMP analysis found most of the methane breakup to occur, $n_e = 7\times10^{18}$ m^{-3} and $T_e = 20$ eV, and launching CH_4, HYDKIN finds that the average lifetimes for $CH_4^+/CH_3^+/CH_2^+/CH^+$ is 0.7/1.4/1.6/2.3 μs for JR and 1.9/2.5/3.3/5.4 μs for EL. The thermalization time for C^+ is 77 μs for this plasma condition, thus a temperature gain can be calculated for the C-atoms of 1.5 eV for JR and 3.2 eV for EL, assuming that every C-atom passed through all four of these HC ion-fragment stages. Since some C-atoms do not pass through all these stages these values are upper limits, but correspond roughly with the values found by DIVIMP, 0.61 and 2.4 eV. HYDKIN also makes clear why the lifetimes are shorter for JR: for example, for CH_4^+, the reaction cross-section for the important dissociative excitation channel $e + CH_4^+ \rightarrow CH_3^+ + H + e$ is ~5× larger in JR than EL; this increase is due to experimental measurements made over the past decade using storage-rings and crossed-beams, as discussed in [2]. In addition, EL do not include four additional dissociative excitation channels for CH_4^+ that JR do, the ones leading to CH_2^+, CH_2, CH^+, and C^+.

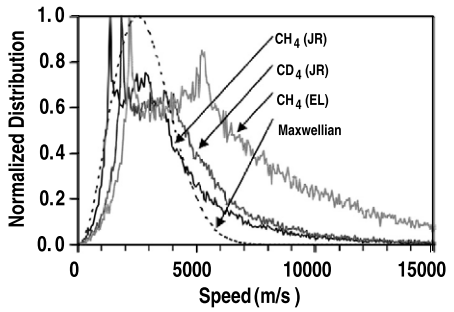

Fig. 4. CI speed distributions resulting from the methane breakup processes for different reaction databases and hydrogen isotope mass. A Maxwellian velocity distribution for $T = 0.4$ eV is shown for reference.

Since the Frank–Condon energy is distributed between the products of each breakup, in inverse proportion to the mass of the fragments, it had been conjectured [6] that the CI line should be about twice as broad for $^{12}CD_4$ as for $^{12}CH_4$. As indicated by Table 1, however, there is little difference in the experimental CI profiles resulting from $^{12}CH_4$ and $^{12}CD_4$ puffing. The code, using JR, was used to compare the $^{12}CD_4$ and $^{12}CH_4$ cases. The average Frank–Condon energy gain per C-atom was found to be 1.17 (0.70) eV for D (H); adding the thermalization heating gave $\langle E_C\rangle = 1.78(1.43)$ eV, i.e. $T_C = 1.19(0.95)$ eV. Taking the representative breakup reaction (i.e. average of CH_n, $n = 1$–4) to be $CH_{2.5} \rightarrow CH_{1.5} + H$ and $CD_{2.5} \rightarrow CD_{1.5} + D$, then based on mass ratios, the D–H *Frank–Condon energy gain* should be in the ratio 2/17 to 1/14.5, i.e. ~1.71, which is, in fact, rather close to the ratio found in the code, 1.17/0.70 = 1.67. However, the *temperature* ratio is closer to unity, 1.19/

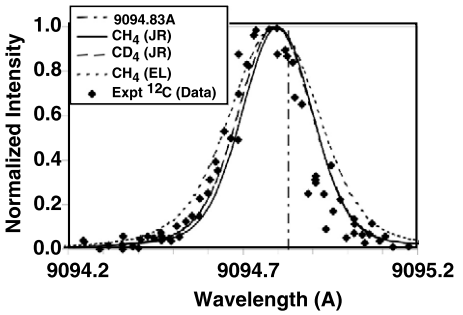

Fig. 5. Changes in the calculated line profiles resulting from different databases for the methane breakup processes and different hydrogen isotope masses. The $^{12}CH_4$ experimental data from Fig. 3 are included for reference. The code-calculated profiles are convolved with the MDS instrument function, see text.

$0.95 \sim 1.25$, and when the effect of the instrument function is included the result is that the computed CI profiles are nearly the same, Fig. 5.

4. Discussion and conclusions

The injection of methane toroidally symmetrically into the crown of a single-null divertor plasma provides what is perhaps the *cleanest* i.e. most readily interpreted and modeled arrangement for assessing in a definitive way whether our present understanding of the breakup kinetics for methane includes the controlling processes. It is important to establish if this is the case in order to provide confidence in the interpretation of the *naturally emitted* CI line wavelength profile, resulting from plasma impact on graphite surfaces, as a means of identifying the relative role of physical and chemical sputtering. In other studies [6–8], methane has been injected into tokamak plasmas through divertor targets or small openings in limiters. Although the latter studies also reported narrow CI profiles, indicative of rather cold C-atoms, the interpretation of such experiments is more difficult and subject to greater uncertainties. First, there is simultaneous sputtering by the plasma ions incident on the solid surfaces adjacent to the point of entry of the methane; this may result, effectively, in two sources of methane. Second, there is greater risk of perturbing the local plasma with such localized injections. Third, plasma interaction with the locally deposited HC layers due to the methane puff itself is a potential complication which has to be accounted for. The DIVIMP code analysis reported here, based on the Janev–Reiter model–database for methane breakup, has produced sufficiently close matches to experimental CI profiles, to provide reasonable confidence that the controlling processes have been identified.

Acknowledgements

This work was supported in part by the US Department of Energy under DE-FC02-04ER54698. The authors would like to acknowledge the support of a Collaborative Research Opportunities Grant from the Natural Sciences and Engineering Research Council of Canada.

References

[1] R.K. Janev, D. Reiter, Phys. Plasmas 9 (2002) 4071;
R.K. Janev, D. Reiter, J. Nucl. Mater. 313–316 (2003) 1202.
[2] R.K. Janev, D. Reiter, Collision processes of hydrocarbon species in hydrogen plasmas: I. The methane family, Report FZ-Jülich Jül -3966, Forschungszentrum Jülich, Jülich Germany (February 2002).
[3] A.B. Ehrhardt, W.D. Langer, Princeton Plasma Physics Laboratory Report PPPL-477 (1987).
[4] W.R. Wampler et al., J. Nucl. Mater., these Proceedings, doi:10.1016/j.jnucmat.2006.12.038.
[5] R.C. Isler, N.H. Brooks, private communication.
[6] P. Bogen, D. Rusbuldt, Nucl. Fusion 32 (1992) 1057.
[7] A.G. McLean et al., J. Nucl. Mater., these Proceedings, doi:10.1016/j.jnucmat.2006.12.062.
[8] N.H. Brooks et al., J. Nucl. Mater., these Proceedings, doi:10.1016/j.jnucmat.2007.01.051.